



# A Monte Carlo study on dose enhancement and photon contamination production by various nanoparticles in electron mode of a medical linac

Mohammad Taghi Bahreyni Toossi,  
Mahdi Ghorbani,  
Leila Sobhkhiz Sabet,  
Fateme Akbari,  
Mohammad Mehrpouyan

**Abstract.** The aim of this study is the evaluation of electron dose enhancement and photon contamination production by various nanoparticles in the electron mode of a medical linac. MCNPX Monte Carlo code was used for simulation of Siemens Primus linac as well as a phantom and a tumor loaded with nanoparticles. Electron dose enhancement by Au, Ag, I and Fe<sub>2</sub>O<sub>3</sub> nanoparticles of 7, 18 and 30 mg/ml concentrations for 8, 12 and 14 MeV electrons was calculated. The increase in photon contamination due to the presence of the nanoparticles was evaluated as well. The above effects were evaluated for 500 keV and 10 keV energy cut-offs defined for electrons and photons. For 500 keV energy cut-off, there was no significant electron dose enhancement. However, for 10 keV energy cut-off, a maximum electron dose enhancement factor of 1.08 was observed for 30 mg/ml of gold nanoparticles with 8 MeV electrons. An increase in photon contamination due to nanoparticles was also observed which existed mainly inside the tumor. A maximum photon dose increase factor of 1.07 was observed inside the tumor with Au nanoparticles. Nanoparticles can be used for the enhancement of electron dose in the electron mode of a linac. Lower energy electron beams, and nanoparticles with higher atomic number, can be of greater benefit in this field. Photons originating from nanoparticles will increase the photon dose inside the tumor, and will be an additional advantage of the use of nanoparticles in radiotherapy with electron beams.

**Key words:** dose enhancement • electron mode • Monte Carlo • nanoparticles • photon contamination

M. T. Bahreyni Toossi, M. Ghorbani  
Medical Physics Research Center,  
Faculty of Medicine,  
Mashhad University of Medical Sciences,  
Mashhad, Iran

F. Akbari<sup>✉</sup>, L. Sobhkhiz Sabet  
Medical Physics Department,  
Reza Radiation Oncology Center,  
Azadeh No. 1, Fallahi No. 2,  
Fallahi Ave., Ghasem Abad, Mashhad, Iran,  
Tel.: +98 51 3522 5673, Fax: +98 51 3522 5671,  
E-mail: f.akbari1@gmail.com

M. Mehrpouyan  
Bioinformatics Research Center,  
Radiology and Radiotherapy Department,  
Faculty of Medicine,  
Sabzevar University of Medical Sciences,  
Sabzevar, Iran

Received: 29 October 2014  
Accepted: 11 June 2015

## Introduction

The aim of radiotherapy is irradiation of a tumor with therapeutic dose, while sparing the surrounding normal tissues. Presence of high atomic number materials such as Au, Gd and I in the tumor will increase the absorption of the radiation inside the tumor. High atomic number materials will increase photoelectric interactions and the resulting photoelectrons, characteristic X-rays and Auger electrons, will increase the tumor dose, locally. The radiation dose depends on the concentration of the high atomic number material. Presence of a high atomic number material inside the target will attenuate the primary radiation, and will thus reduce the dose outside the target. High atomic number materials can be designed in the form of nanoparticles so that they can be absorbed mainly by the tumor cells [1].

Due to higher metabolism in the tumor cells, and higher abundance of vessels inside the tumor compared to normal tissues, the tumor absorbs the nanoparticles, which are relatively larger molecules in comparison to other biological molecules present in tissue vessels, at a higher level [2].

Dose enhancement by nanoparticles in combination with brachytherapy sources, or external beams from medical linacs, has been the subject of various studies [2–6]. Zhang *et al.* [4] have evaluated dose enhancement by gold nanoparticles. They have used Geant4 Monte Carlo code, and simulated an  $^{192}\text{Ir}$  source in a water phantom. It was observed that nanoparticles with concentration of  $10^{15}$  particles per  $\text{cm}^3$  will provide a dose enhancement of 60% in the tumor. Cho *et al.* [6] have calculated the tumor dose enhancement factor for gold nanoparticles with different concentrations by means of the Monte Carlo code. The MCNPX code was used for simulation of  $^{137}\text{Cs}$ ,  $^{192}\text{Ir}$ ,  $^{125}\text{I}$  and  $^{105}\text{Pd}$  sources. The dose enhancement factors for these sources were obtained as high as 1.03, 1.11, 3.43 and 2.17, respectively. Chow *et al.* [7] in a Monte Carlo simulation study have studied the production of secondary electrons originating from gold nanoparticles when irradiated by monoenergetic electron beams. Spherical nanoparticles with 2, 50 and 100 nm diameters in a water phantom were irradiated by 50 keV, 250 keV, 1 MeV and 4 MeV monoenergetic electrons. The Geant4 code was utilized in the simulations, and the energy of the secondary electrons originating from gold nanoparticles was determined. The results have indicated that the average effective range of the secondary electrons was larger for gold nanoparticles of larger sizes, as well as for higher energy electrons. For electron energies and gold nanoparticle sizes in this study, the average effective range of the secondary electrons outside the nanoparticle was 0.5–15  $\mu\text{m}$ . This value is in the size range of a living cell.

Rahman *et al.* [8] have used polymer gel containing gold nanoparticles for measurement of dose enhancement for synchrotron X-rays as well as electron and photon beams. nPAG gel was applied for 3-D dosimetry in radiotherapy. The samples were irradiated with X-rays of various energies, and 6 MeV electron beams of a linac. Analysis of dose-response curves has implied that a dose enhancement factor of 1.37 for gold nanoparticles irradiated with the electron beam has been observed. Rahman *et al.* [9] have used gold nanoparticles in another study for enhancement of cell damage by irradiation of bovine aortic endothelial cells by use of superficial X-rays and megavoltage electron beams. With an increase in the concentration of gold nanoparticles, the cell damage has shown to increase. For 1 mM concentration of gold nanoparticles with kilovoltage X-ray beam, the enhancement peaked at 25 times. Similar, but to a lesser extent effects were observed for electron beams. The results have implied that gold nanoparticles can be used to enhance the effect of absorbed doses for both kilovoltage X-rays and megavoltage electron radiation therapy beams. It was concluded that the enhancement effect can be used in the future for local control improvement in various treatment modalities using kilovoltage X-rays or megavoltage electron beams. Based on our investigations there are few studies on dose enhancement by nanoparticles in electron beams.

Bremsstrahlung photons are produced by the interaction of electrons with various components

of the head of a linac including the exit window, scattering foils, collimators and electron applicators [10]. Such particles are accounted for as photon contamination in electron beams. It is predicted that these photons are produced by the presence of nanoparticles in phantom, when the nanoparticles are irradiated by electron beams. This may be due to the interaction of electrons with nanoparticles inside the phantom through bremsstrahlung interactions. Photon contamination in electron beams was the topic of research for a number of previous studies [11–14]. However, because of the difference in electron energy spectrum, the composition and geometry of the head components, and the relative position of the components, the amount of photon contamination is different from one linac to the other [13]. Furthermore, presence of nanoparticles in the tumor in a phantom can result in an increase in photon contamination in electron mode of a medical linac.

Concluding from the above mentioned studies, some focused on electron dose enhancement, others on photon contamination of the linac's head components. But to the best of our knowledge there is no study available on electron dose enhancement and photon contamination production by various nanoparticles. The aim of this study is evaluation of electron dose enhancement due to the presence of Au, Ag, I and  $\text{Fe}_2\text{O}_3$  nanoparticles in the tumor for 8, 12 and 14 MeV electron beams of a linac. Then, the amount of increase in photon contamination due to various types of nanoparticles is calculated through Monte Carlo simulations.

## Materials and methods

### Simulation of Siemens Primus linac

Our simulation of the Siemens Primus linac's head was based on a previous study by the authors in which the linac was simulated in 8, 12 and 14 MeV electron energies [15]. In that study, MCNPX Monte Carlo code was used and the benchmark was performed by comparison of the simulation percentage depth dose data of 10 cm  $\times$  10 cm, 15 cm  $\times$  15 cm and 30 cm  $\times$  30 cm applicators, with the corresponding measured data. The comparisons were based on gamma index calculations, and the gamma index value was less than unity in most of the data points. In gamma function calculations, dose difference and distance to agreement criteria were 3% and 2 mm, respectively [15]. The same criteria were also used in other studies in the field of radiotherapy [16]. Gamma value of equal to or less than 1.00 means that the two dose data sets are in agreement. The mentioned study indicates the agreement of the data of our Monte Carlo model of the Siemens Primus linac in 8, 12 and 14 MeV electron energies with the measured values [15]. The simulation model of the linac's head in electron mode, which has been verified in Ref. [15], has been used here-in for evaluation of electron dose enhancement and photon contamination production in presence of various nanoparticles in tumor.

### Electron dose enhancement calculations

MCNPX Monte Carlo code (ver. 2.4.0) [17] was used in simulation of the linac's head, phantom, tumor and nanoparticles. Electron dose enhancement was calculated for 8, 12 and 14 MeV electrons for a 10 cm × 10 cm applicator. A cylindrical phantom with 15 cm radius and a 30 cm height was defined in the simulations, and a 2 cm × 2 cm × 1 cm tumor was positioned on the central axis of the beam. The height of the tumor was 1 cm, while its width and length were 2 cm. Source to surface distance (SSD) was defined as 80 cm in the simulations. The chemical composition of the phantom was soft tissue with four elements as defined by report No. 44 of International Commission on Radiation Units and Measurements (ICRU): 76.2% oxygen, 10.1% hydrogen, 11.1% carbon and 2.6% nitrogen [18]. Since the depth of build-up depends on the electron beam energy, the position of the tumor was defined differently based on the energy of the electrons. The depth of the tumor was 2 cm for 8 MeV, 3 cm for 12 MeV and 3.5 cm for 14 MeV electron beams. Selection of these tumor depths for these electron energies was based on the percentage depth dose curves of the electron beams. In other words, the relative dose decreases abruptly beyond the 90% percentage depth dose level, therefore, the useful treatment depth for electron beam is depth of 90% percentage dose. It is obvious that this depth depends on the electron energy. A schematic diagram showing the simulation geometry is presented in Fig. 1. The center of the tumor was positioned on the central axis of the beam. The electron dose enhancement was calculated for Au, Ag, I and Fe<sub>2</sub>O<sub>3</sub> nanoparticles. The selection of these nanoparticles for dose enhancement purpose was based on previous studies with these agents on dose enhancement [3, 19–21]. While, iodine was used as dose enhancement [20], not as nanoparticle form, but it can be made as nanoparticles. For this purpose, the nanoparticles were defined in the tumor volume as uniform mixture by the soft tissue. Nanoparticles with concentrations of 7, 18 and 30 mg/ml were evaluated separately in various simulations. The effect of the electrons' and photons' energy cut-off on electron dose enhancement was evaluated. Electron dose enhancement with energy cut-off of 500 keV was calculated for 7, 18 and 30 mg/ml concentrations. With 10 keV energy cut-off, dose enhancement factor was calculated only for the 30 mg/ml concentration. Density and composition of the tumor was modified in the simulations to include the mixture of nanoparticles and soft tissue.

The absorbed dose in various depths inside the phantom and tumor was calculated in two conditions: with presence of nanoparticles inside the tumor, and without them. Dose values were calculated in cubic cells located on the beam's central axis inside the phantom. Dose enhancement factor (DEF) was then calculated as the ratio of dose in a voxel in case of presence of nanoparticles in the tumor to that in the absence of nanoparticles. DEF was averaged over the voxels inside the tumor, and

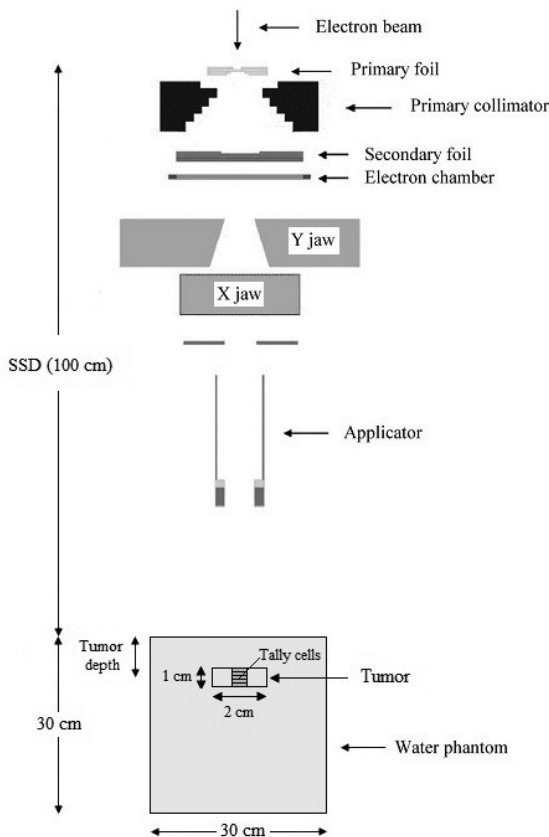


**Fig. 1.** Geometry of head of Siemens Primus linac in electron mode as well as the water phantom.

the average value was reported. Variation of DEF with the type of nanoparticles, concentration of the nanoparticles, electron energy and energy cut-off was considered, and discussed.

Energy cut-off and cell importance was the variance reduction methods used. Cell importance for both electrons and photons was set as 1 for all the program cells, while it was defined equal to 100 in the tally cells inside the phantom. The number of electrons transported was  $2 \times 10^8$ . \*F8 tally was used for calculation of electron dose, and the tally value was divided by the mass of the tally cell to obtain the energy deposition per unit mass of the tally voxel. The tally voxels were 2 mm × 2 mm × 2 mm, located on the central axis of the beam from 2 mm to 6.6 cm depths in the soft tissue phantom. The maximum value of the Monte Carlo statistical error was 6.27% in these simulations. An input file for 1 keV energy cut-off, 30 mg/ml Au nanoparticles with 14 MeV electrons were run as well and the electron DEF was calculated and compared with the data for other energy cut-offs. Other details of this simulation were the same as the above mentioned method for the other energy cut-offs.

### Photon contamination calculations

The simulation geometry including head components, geometry and location of the tumor, types of nanoparticles, electron energies and so on was the same as that described above for electron dose enhancement

evaluation. However, there were minor differences which are described here. For photon contamination calculation, F6 tally for photons was scored in the tally cells. The number of electron histories followed was  $1.5 \times 10^8$ . The maximum value of the Monte Carlo type A uncertainty was 5.59% which was related to the cells outside the tumor. Type A uncertainties in Monte Carlo calculations for the cells inside the tumor or voxels at superficial cells inside the phantom were less than this level. Photon dose was obtained in the tally cells for two cases: presence of nanoparticles in the tumor, and in the absence of them. The ratio of the photon dose from the first case to that from the second case was calculated and reported as the 'photon dose increase factor'. The factor was averaged in the tally cells, on the beam's central axis inside the tumor and was reported for various nanoparticle types, concentrations, electron energies and energy cut-offs. The ratio was also obtained for various depths in the phantom, ranging from 2 mm to 6.6 cm.

**Table 1.** Electron dose enhancement factor for various nanoparticles with energy cut-off of 500 keV. The values are averages on the beam's central axis inside the tumor

Type of NPs	Electron energy [MeV]								
	8			12			14		
	Concentration [mg/ml]								
	7	18	30	7	18	30	7	18	30
Au	1.01	1.01	1.02	1.00	1.01	1.02	1.00	1.01	1.02
Ag	1.00	1.00	1.02	1.00	1.00	1.01	1.00	1.01	1.01
I	1.00	1.00	1.00	1.00	1.01	1.01	1.00	1.01	1.01
Fe <sub>2</sub> O <sub>3</sub>	1.00	1.00	1.00	1.00	1.00	1.00	1.00	1.00	1.00

**Table 2.** Electron dose enhancement factor for various nanoparticles with 30 mg/ml concentration for energy cut-off of 10 keV. The values are DEF on the beam's central axis inside the tumor

Type of NPs	Electron energy [MeV]		
	8	12	14
Au	1.09 ± 0.03	1.07 ± 0.02	1.06 ± 0.02
	1.08 ± 0.03	1.07 ± 0.02	1.05 ± 0.02
	1.08 ± 0.03	1.06 ± 0.02	1.05 ± 0.01
	1.07 ± 0.03	1.06 ± 0.02	1.05 ± 0.01
	1.07 ± 0.03	1.05 ± 0.02	1.04 ± 0.01
Average DEF ± average uncertainty	1.08 ± 0.03	1.06 ± 0.02	1.05 ± 0.01
Ag	1.06 ± 0.03	1.04 ± 0.02	1.03 ± 0.01
	1.05 ± 0.03	1.03 ± 0.02	1.02 ± 0.01
	1.05 ± 0.03	1.04 ± 0.02	1.02 ± 0.01
	1.04 ± 0.03	1.03 ± 0.02	1.02 ± 0.01
	1.04 ± 0.03	1.03 ± 0.02	1.01 ± 0.01
Average DEF ± average uncertainty	1.05 ± 0.03	1.03 ± 0.02	1.02 ± 0.01
I	1.04 ± 0.03	1.04 ± 0.02	1.04 ± 0.01
	1.04 ± 0.03	1.03 ± 0.02	1.03 ± 0.01
	1.04 ± 0.03	1.03 ± 0.02	1.03 ± 0.01
	1.04 ± 0.03	1.03 ± 0.02	1.02 ± 0.01
	1.03 ± 0.03	1.03 ± 0.02	1.02 ± 0.01
Average DEF ± average uncertainty	1.04 ± 0.03	1.03 ± 0.02	1.03 ± 0.01
Fe <sub>2</sub> O <sub>3</sub>	0.99 ± 0.03	1.00 ± 0.02	1.00 ± 0.01
	1.00 ± 0.03	1.00 ± 0.02	1.00 ± 0.01
	1.00 ± 0.03	0.99 ± 0.02	0.99 ± 0.01
	1.00 ± 0.03	0.99 ± 0.02	1.00 ± 0.01
	0.99 ± 0.03	1.00 ± 0.02	0.99 ± 0.01
Average DEF ± average uncertainty	1.00 ± 0.03	1.00 ± 0.02	1.00 ± 0.01

## Results

### Electron dose enhancement factors

Electron dose enhancement factors by Au, Ag, I and Fe<sub>2</sub>O<sub>3</sub> nanoparticles with 7, 18 and 30 mg/ml concentrations with 500 keV energy cut-off are listed in Table 1. Electron dose enhancement factors by Au, Ag, I and Fe<sub>2</sub>O<sub>3</sub> nanoparticles with 30 mg/ml concentrations with 10 keV energy cut-off are listed in Table 2.

As is evident from the data shown in Table 1 and Table 2, electron dose enhancement is not considerable when the energy cut-off of 500 keV is defined for electrons and photons. However, the electron dose enhancement factor amounts to as high as 1.08, when the energy cut-off is 10 keV. Minimum electron dose enhancement factor outside the tumor with 10 keV energy cut-off was 0.92. With the definition of 1 keV energy cut-off, for 14 MeV electrons, the average dose enhancement factor in the tumor in

**Table 3.** Dose increase factor for photon contamination in the tumor in the presence of various nanoparticles. The values are the average values on the beam's central axis inside the tumor. The values are related to 500 keV energy cut-off

Type of NPs	Electron energy [MeV]								
	8			12			14		
	Concentration [mg/ml]								
	7	18	30	7	18	30	7	18	30
Au	1.00	1.01	1.01	1.00	1.01	1.02	1.00	1.01	1.02
Ag	0.99	1.00	1.00	1.00	1.00	1.01	1.00	1.01	1.01
I	1.00	1.00	1.00	1.00	1.00	1.01	1.00	1.01	1.01
Fe <sub>2</sub> O <sub>3</sub>	1.00	1.00	1.00	1.02	1.00	1.00	1.00	1.00	1.00

the presence of Au with 30 mg/ml concentrations was obtained as 1.06.

### Photon contamination results

The photon contamination increasing factors in the tumor in the presence of Au, Ag, I and Fe<sub>2</sub>O<sub>3</sub> nanoparticles with 7, 18 and 30 mg/ml concentrations with 500 keV energy cut-off are listed in Table 3. The photon contamination increasing factors in the tumor in the presence of Au, Ag, I and Fe<sub>2</sub>O<sub>3</sub> nanoparticles with 30 mg/ml concentration for 10 keV energy cut-off are listed in Table 4. Minimum photon contamination increase factor outside the tumor with 10 keV energy cut-off was equal to 0.98.

### Discussion

In the present study, electron dose enhancement and photon contamination production in the presence of various nanoparticles were evaluated in electron mode of a medical linac. Among all the situations evaluated, the highest electron dose enhancement obtained was 1.08, which was that of 30 mg/ml Au nanoparticles with 8 MeV electron beams (Table 2). Although this level of dose enhancement is not as high as the levels obtained by brachytherapy photon sources in previous studies [3, 6, 22], it seems to be a clinically significant value, because it corresponds to an 8% dose enhancement inside the tumor. The fact that the observed dose enhancement for electron beam therapy is lower than brachytherapy depends on the voxelization adopted in these two modalities. Nowadays, these therapeutic electron energies are available in most of the radiotherapy departments.

**Table 4.** Dose increase factor for photon contamination in the tumor in the presence of various nanoparticles. The values are the average values on the beam's central axis inside the tumor. The values are related to 10 keV energy cut-off and concentration of 30 mg/ml

Type of NPs	Electron energy [MeV]		
	8	12	14
Au	1.07	1.07	1.06
Ag	1.04	1.05	1.04
I	1.02	1.03	1.03
Fe <sub>2</sub> O <sub>3</sub>	1.00	1.00	1.02

An interpretation of the electron dose enhancements in Table 2 considering the related uncertainties is useful. Based on the data presented in this table, in the cases that there is an electron dose enhancement, the dose enhancement level is higher than the related uncertainty. As an example, for 8 MeV electron with 30 mg/ml Au nanoparticles, the DEF is 1.08. This amounts to 8% dose enhancement with the related uncertainty being 3%. Therefore, in most of the cases the dose enhancements are meaningful, some exceptions are when the DEF is 1.00.

As it was mentioned in the results, the minimum electron dose enhancement factor outside the tumor with 10 keV energy cut-off was 0.92. As a consequence, the dose outside the tumor decreases when the nanoparticles are introduced inside the tumor. While this seems to be a beneficial effect, results might be changed with another energy cut-off. In other words, the electron dose enhancement factor outside the tumor could be evaluated for various nanoparticles and electron beams with lower electron energy cut-offs.

In electron beam therapy, the dose enhancement is local to the nanoparticle, therefore dose enhancement averaging over a micro-sized voxel can change the results of the study. This is only a physical point of view. From biological aspect, additional to the dose increase, there are other criteria which have importance in the cellular damage: the range of the secondary electrons, the location of the nanoparticles in the cells and so on. These effects are dependent on the electron beam energy as well as the type and concentration of the nanoparticles. In other words, the dose enhancement distribution at nano/micro level is fundamental to link the physical phenomena to the radiobiological effects of the electron beams. Therefore, dose enhancement study in electron beam therapy at micro- and nano-scale would be interesting as a future evaluation in this field.

With a 10 keV energy cut-off (Table 4), dose increase factor inside the tumor for photon contamination is higher than 1.00 in most cases. A value of higher than 1.00 in this case implies that the photon contamination has increased inside the tumor. The dose increase factor in this case has a maximum value of 1.07 for 30 mg/ml Au nanoparticles in 8 MeV and 12 MeV electron energies. This level amounts to a 7% increase in photon contamination inside the tumor. Photon contamination may not be useful in its general concept in electron mode of a linac, but its increase inside the tumor in the presence

of nanoparticles will be an advantage. Increase in photon contamination in a tumor in electron mode can be seen by another point of view. In other words, this increase can be a result of the particle induced X-ray emission (PIXE) effect. In this method, when metallic nanoparticles are irradiated by high energy charged particles or heavy ions, they release X-rays or gamma-rays due the particle induced X-ray emission or particle induced gamma-ray emission (PIGE) effect [23]. The consequent phenomenon is emission of Auger electrons which enhances local tumor dose, as an advantage.

The dose increase factor for photon contamination outside the tumor is equal to or less than 1.00 in most data points. This is another advantage of the presence of nanoparticles in the tumor and implies the fact that the produced photons in presence of nanoparticles are absorbed in short distances in soft tissue.

From the data presented in Tables 1 and 2, it can be noticed that the electron dose enhancement factor is higher when 10 keV energy cut-off is used for photons and electrons in the simulations. This effect indicates that lower energy electrons have more of a contribution in dose enhancement by electrons, because when they are not neglected in the simulations, the DEF value for electrons shows a higher level. Among the DEF values with 500 keV and 10 keV energy cut-offs, those with 10 keV seem to be more close to the real value, because in a real situation, the low energy electrons contribute to the absorbed dose in a voxel.

The data in Tables 1 and 3 (for various situations including type of nanoparticles, concentration and electron energies) in most of the cases are equal or close to 1.00. The data in these two tables indicate that with 500 keV cut-off no significant electron dose enhancement or photon contamination enhancement is observed inside the tumor.

With 500 keV energy cut-off, the dose enhancements for Au, Ag, I and Fe<sub>2</sub>O<sub>3</sub> nanoparticles are relatively similar and in most cases equal to 1.00. However, with 10 keV energy cut-off, the electron dose enhancement factor, and the dose increase in photon contamination is higher for Au and Ag nanoparticles, respectively, compared to those of I and Fe<sub>2</sub>O<sub>3</sub>. While the DEFs for I are higher than 1.00, the values for Fe<sub>2</sub>O<sub>3</sub> are in almost all cases equal to 1.00. Based on these results, use of Fe<sub>2</sub>O<sub>3</sub> for dose enhancement in electron mode has no justification. Of course, this result is from a physical point of view, and the biological issue is another concern which cannot be ignored. When considering atomic numbers of the nanoparticles (79 for Au, 47 for Ag, 53 for I and 15.2 for Fe<sub>2</sub>O<sub>3</sub>, estimated average number) it cannot be generally concluded that the DEF is directly proportional to the atomic number of the nanoparticles. However, Au and Fe<sub>2</sub>O<sub>3</sub> with the highest and lowest atomic numbers, respectively, have the highest and lowest values of DEF.

Looking at the DEF data for various energies, the DEF for 8 MeV electrons with a definition of 10 keV energy cut-off (Table 2) is higher than those of other energies. Ignoring some exceptions, it can

be mentioned that DEF is higher in lower energy electron beams.

As it was mentioned in the results section, with a definition of 1 keV energy cut-off, the electron dose enhancements in the tumor in the presence of Au with 30 mg/ml concentrations for 14 MeV electrons was 1.06. This value can be compared with the corresponding value in this case for 10 keV cut-off which is equal to 1.05. According to these DEF values, it can be concluded that 10 keV and 1 keV energy cut-offs show relatively the same dose enhancements. However, it should be noted that the latter would need a longer Monte Carlo calculation time. For example, the time needed for 150 million electrons with 1 keV energy cut-off was 8 times more than 10 keV, therefore computers with high processing powers are necessary tools for this purpose. Relatively the same dose enhancement results are obtained for these energy cut-offs. As low energy electrons take an important role in deoxyribonucleic acid (DNA) damage, investigation on electron energy cut-off down to the eV scale and the related DNA damages may show stronger dependence on the electron energy cut-off. Geant4 Monte Carlo code is capable of tracking such interactions.

The electron dose enhancements obtained in this study are not much higher from the increase in the physical energy deposition inside the voxels from a tumor point of view. However, it should be noted that the biological effects do not depend only on the absorbed dose. In other words, when one considers the biological effects, the interpretation of these levels of dose enhancements may be different. In order to assess the biological effects, applying a radiobiological model on the effectiveness of nanoparticles in electron beam radiotherapy is suggested.

Based on the data shown in tables (Table 1 and Table 3), no significant trend in electron dose enhancement and photon contamination enhancement was observed with an increase of the concentration of nanoparticles. It should be noted that the data in these tables are those for various concentrations with 500 keV energy cut-off. However, the DEFs in Table 2 and dose increase factors in Table 4, with 10 keV energy cut-off, are related to 30 mg/ml concentrations of nanoparticles.

DEF depends on the electron energy spectrum, whereas electron energy distribution depends on the depth of the tumor. Calculated DEFs in this work are geometry specific. To perform an analysis on dependence of dose enhancement on the electron energy spectrum and depth of tumor, calculation of energy spectra at different depths as well as investigation of the relation between DEF and tumor depth would be valuable.

There is no similar study on physical dose enhancement in clinical electron beams, to compare the present results. In the present study, 2 mm × 2 mm × 2 mm voxels were used in dose calculations. Bakhshabadi *et al.* [24] defined cells with 1 mm thickness as the tally cells in photon activation therapy. In photon activation therapy the dose due to secondary particles (Auger electrons) are the most responsible for the biological effect, in some extent

similar to the present study in which the secondary electrons are important. Rahman *et al.* [8] used 2 mm slice thickness for magnetic resonance imaging (MRI) analysis of gel samples in an experimental measurement of radiation dose enhancement in 6 MeV electron beam. However, it should be noted that the dose enhancement of nanoparticles in an electron beam irradiation is typically local to them (this happens because of the enhanced production of low energy electrons) and the dose enhancement changes significantly in a sub-mm range. Therefore, an investigation on the effect of lower voxel sizes on dose enhancement can be of interest and dose enhancement distribution at nano/micro level is fundamental to link the physical to the radiobiological effect of radiation as pointed out by McMahon *et al.* [25]. Production of secondary electrons from a nanoparticle increases by 10 to 2000 fold compared to the situation of absence of GNP in irradiation of nanoparticles with photon beams. Additionally, the mean effective range of electron tracks in 50 kVp to 6 MV photon beam irradiation ranges from  $\sim 3 \mu\text{m}$  to 1 mm [26]. However, we could not find a study on the range of secondary electrons when a nanoparticle is irradiated by an electron beam, and this evaluation would be useful in further investigations in this field.

## Conclusions

Lower energy beams (8 MeV) and nanoparticles with higher atomic numbers (especially Au NPs) show higher levels of dose enhancement, and thus can be of higher benefit in this regard. Among the four types of nanoparticles used, Au and Ag nanoparticles show relatively significant dose enhancement, and are proposed for enhancing the electron dose in the electron mode of a medical linac. Photons originating from interaction of electrons with nanoparticles will increase the photon dose inside the tumor and can be considered as another advantage of the use of nanoparticles in radiotherapy with electron beams.

Based on the results for 50 and 10 keV energy cut-offs defined, it is obvious that low energy electrons are the main source of electron tumor dose enhancement. The electron dose enhancement has been calculated for 10 keV energy cut-off, but it is predicted that lower energy electrons with energies lower than 10 keV may have higher contribution in dose enhancement. Furthermore, in our Monte Carlo simulations in the present study, atomic distribution was used to define the composition of the tumor including nanoparticles. More precisely, definition of nanoparticles will be specification of them as nanospheres by use of lattice option in the MCNP code. A previous study by Ghorbani *et al.* [27] on gold nanoparticles and gamma emitting brachytherapy sources has shown that the method for definition of nanoparticles in the Monte Carlo program will affect the DEF values. These effects are called as future studies in the field of dose enhancement by nanoparticles in radiotherapy with electron beams.

**Acknowledgments.** This work was performed in Mashhad, Iran. The authors would like to thank and express their appreciation to Mashhad University of Medical Sciences (MUMS) for the financial support of this work.

## References

1. McMahon, S., Mendenhall, M., & Jain, S. (2008). Radiotherapy in the presence of contrast agents: a general figure of merit and its application to gold nanoparticles. *Phys. Med. Biol.*, 53(20), 5635–5651. DOI: 10.1088/0031-9155/53/20/005.
2. Ghasemi, M. R., Zafarghandi, M., & Raisali, G. (2010). Monte Carlo simulation of dose absorption of nano-particles-labeled tissues used in x-ray microbeam radiation therapy. *J. Nucl. Sci. Technol.*, 50(4), 37–47.
3. Cho, S. (2005). Estimation of tumour dose enhancement due to gold nanoparticles during typical radiation treatments: a preliminary Monte Carlo study. *Phys. Med. Biol.*, 50(15), 163–173. DOI: 10.1088/0031-9155/50/15/N01.
4. Zhang, S. X., Gao, J., & Buchholz, T. A. (2009). Quantifying tumour-selective radiation dose enhancements using gold nanoparticles: a Monte Carlo simulation study. *Biomed. Microdevices*, 11(4), 925–933. DOI: 10.1007/s10544-009-9309-5.
5. Khatib, E., Scrimger, J., & Murray, B. (1991). Reduction of the bremsstrahlung component of clinical electron beams: implications for electron arc therapy and total skin electron irradiation. *Phys. Med. Biol.*, 36(1), 111–118. DOI: 10.1088/0031-9155/36/1/010.
6. Cho, S., Jong, H., & Chan, H. (2010). Monte Carlo simulation study on dose enhancement by gold nanoparticles in brachytherapy. *J. Korean Phys. Soc.*, 56(6), 1754–1758. DOI: 10.3938/jkps.56.1754.
7. Chow, J. C., Leung, M. K., & Jaffray, D. A. (2012). Monte Carlo simulation on a gold nanoparticle irradiated by electron beams. *Phys. Med. Biol.*, 57(11), 3323–3331. DOI: 10.1088/0031-9155/57/11/3323.
8. Rahman, W. N., Wong, C. J., & Ackerly, T. (2012). Polymer gels impregnated with gold nanoparticles implemented for measurements of radiation dose enhancement in synchrotron and conventional radiotherapy type beams. *Australas. Phys. Eng. Sci. Med.*, 35(3), 301–309. DOI: 10.1007/s13246-012-0157-x.
9. Rahman, W. N., Bishara, N., & Ackerly, T. (2009). Enhancement of radiation effects by gold nanoparticles for superficial radiation therapy. *Nanomedicine*, 5(2), 136–142. <http://dx.doi.org/10.1016/j.nano.2009.01.014>.
10. Jabari, N., & Hashemi, B. (2009). An assessment of the photon contamination due to bremsstrahlung radiation in the electron beams of a Neptun 10PC linac using a Monte Carlo method. *Iran. J. Med. Phys.*, 6(1), 21–32.
11. Mahdavi, M., Mahdavi, S. R. M., & Alijanzadeh, H. (2011). Comparing the measurement value of photon contamination absorbed dose in electron beam field for Varian clinical accelerator. *IUP J. Phys.*, 5(3), 7–11.
12. Sharma, A. K., Supe, S. S., & Anantha, N. (1995). Physical characteristics of photon and electron beams from a dual energy linear accelerator. *Med. Dosim.*, 20(1), 55–66. DOI: 10.1016/0958-3947(94)00019-F.
13. Gur, D., Bukovitz, A. G., & Serago, C. (1979). Photon contamination in 8-20-MeV electron beams from a linear accelerator. *Med. Phys.*, 6(2), 145–146. DOI: 10.1118/1.594525.

14. Bruno, B., Hyodynmaa, S., & Brahme, A. (1997). Quantification of mean energy and photon contamination for accurate dosimetry of high-energy electron beams. *Phys. Med. Biol.*, *42*(10), 1849–1873. DOI: 10.1088/0031-9155/42/10/001.
15. Bahreyni Toossi, M. T., Ghorbani, M., & Akbari, F. (2013). Monte Carlo modeling of electron modes of a Siemens Primus linac (8, 12 and 14 MeV). *J. Radiother. Pract.*, *12*(4), 352–359. DOI: 10.1017/S1460396912000593.
16. Reich, P. D. (2008). *A theoretical evaluation of transmission dosimetry in 3D conformal radiotherapy*. Doctoral dissertation, Adelaide University of Australia. Retrieved 17 March 2015, from <https://digital.library.adelaide.edu.au/dspace/bitstream/2440>.
17. Waters, L. S. (2002). *MCNPX User's Manual, Version 2.4.0*. Los Alamos National Laboratory (LAC-CP-02-408).
18. ICRU. (1989). *Tissue substitutes in radiation dosimetry and measurement*. Bethesda, MD: ICRU (ICRU Report No. 44).
19. Guidelli, E. J., & Baffa, O. (2014). Influence of photon beam energy on the dose enhancement factor caused by gold and silver nanoparticles: An experimental approach. *Med. Phys.*, *41*(3), 032101. DOI: 10.1118/1.4865809.
20. Iwamoto, K. S., Cochran, S. T., & Winter, J. (1987). Radiation dose enhancement therapy with iodine in rabbit VX-2 brain tumors. *Radiother. Oncol.*, *8*(2), 161–170. [http://dx.doi.org/10.1016/S0167-8140\(87\)80170-6](http://dx.doi.org/10.1016/S0167-8140(87)80170-6).
21. Klein, S., Sommer, A., & Distel, L. (2014). Superparamagnetic iron oxide nanoparticles as novel x-ray enhancer for low-dose radiation therapy. *J. Phys. Chem. B.*, *118*(23), 6159–6166. DOI: 10.1021/jp5026224.
22. Roeske, J. C., Nunez, L., & Hoggarth, M. (2007). Characterization of the theoretical radiation dose enhancement from nanoparticles. *Technol. Cancer Res. Treat.*, *6*(5), 395–401.
23. Kim, J. K., Seo, S. J., & Kim, K. H. (2010). Therapeutic application of metallic nanoparticles combined with particle-induced x-ray emission effect. *Nanotechnology*, *21*(42), 425102. DOI: 10.1088/0957-4484/21/42/425102.
24. Bakhshabadi, M., Ghorbani, M., & Soleimani Meigoni, A. (2013). Photon activation therapy: a Monte Carlo study on dose enhancement by various sources and activation media. *Australas. Phys. Eng. Sci. Med.*, *36*(3), 301–311. DOI: 10.1007/s13246-013-0214-0.
25. McMahan, S. J., Hyland, W. B., & Muir, M. F. (2011). Biological consequences of nanoscale energy deposition near irradiated heavy atom nanoparticles. *Sci. Rep.*, *1*(18), 1–9. DOI: 10.1038/srep00018.
26. Leung, M. K. K., Chow, J. C. C., & Chithrani, B. (2011). Irradiation of gold nanoparticles by x-rays: Monte Carlo simulation of dose enhancements and the spatial properties of the secondary electrons production. *Med. Phys.*, *38*(2), 624–631. DOI: 10.1118/1.3539623.
27. Ghorbani, M., Pakravan, D., & Bakhshabadi, M. (2012). Dose enhancement in brachytherapy in the presence of gold nanoparticles: a Monte Carlo study on the size of gold nanoparticles and method of modeling. *Nukleonika*, *57*(3), 401–406.